Electrochimica Acta 112 (2013) 371–377

Contents lists available at ScienceDirect

Electrochimica Acta

journal homepage: www.elsevier.com/locate/electacta

The electronic structure characterization of oxide film on bulk nanocrystalline 304 stainless teel in hydrochloric acid solution

S.G. Wang[a,b,c,*], M. Sun[a,b], K. Long[b], Z.D. Zhang[a,b,c]

[a] Shenyang National Laboratory for Material Sciences, Chinese Academy of Sciences, 72 Wenhua Road, 110016 Shenyang, PR China
[b] Institute of Metal Research, Chinese Academy of Sciences, 72 Wenhua Road, 110016 Shenyang, PR China
[c] International Centre for Materials Physics, Chinese Academy of Sciences, 72 Wenhua Road, 110016 Shenyang, PR China

ARTICLE INFO

Article history:
Received 2 August 2013
Received in revised form 2 September 2013
Accepted 2 September 2013
Available online 9 September 2013

Keywords:
Stainless steel
Oxide film
XPS
SEM
Pitting corrosion

ABSTRACT

The electronic structures and compositions of the two oxide films on bulk nanocrystalline 304 stainless steel (BN-SS304) and its conventional polycrystalline counterpart (CP-SS304) after 30 days' immersion test in 0.5 mol/L HCl solution at room temperature were studied by X-ray photoelectron spectroscopy. The enhanced uniform and pitting corrosion resistances of BN-SS304 were attributed to the larger resistance and better chemical stability of the oxide film on BN-SS304, the less corrosion rate of Cr^0 for BN-SS304 and the larger atomic percentage of Cr^{3+} in the oxide film on BN-SS304. The larger resistance of oxide film on BN-SS304 resulted from the less state densities of valence electrons around Fermi level in the oxide film on BN-SS304. The better chemical stability of oxide film on BN-SS304 was attributed to (1) the larger binding energies of Fe^{2+} 2p3/2, Fe^{3+} 2p3/2 and Cr^{3+} 2p3/2 in the oxide film on BN-SS304; (2) the larger atomic percentages of Cr^{3+} and Fe^{2+} in the oxide film on BN-SS304.

© 2013 Elsevier Ltd. All rights reserved.

1. Introduction

The corrosion properties of metal materials were usually studied by scanning electron microscope (SEM), X-ray diffraction, potentiodynamic polarization [1], electrochemical impedance spectrum [2], Scanning Kelvin probe [3], atomic force microscope [4] and X-ray photoelectron spectroscopy (XPS) [5–7] etc. The corrosion properties of stainless steels have been extensively studied due to their wide application with good mechanical properties and corrosion resistances [8,9]. XPS has been used to determine the in-depth chemical composition, chemical shifts of elements and valence electron bands of oxide films [10–13]. It has been found that the structures and chemical composition of oxide film on stainless steel can affect the reactivity, adhesion, cohesion properties and corrosion resistance of stainless steel. The XPS characterization for the oxide films on 304 stainless steel under different dissolved oxygen concentrations in 290 °C water was carried out, the relative Cr content in the oxide film on 304 stainless steel decreased while relative Ni content increased [14]. The compositions of oxide films on AISI 316L, Co–28Cr–6Mo and Ti–6Al–4V alloys exposed to phosphate buffered solutions were also identified by XPS, the high Cr concentrations in oxide layers on 316L and Co–Cr–Mo corresponded with the slow dissolution rate of Cr compared to other alloying elements of 316L and Co–28Cr–6Mo alloys [15]. The XPS analysis of the oxide films on 304 stainless steel in rolled and heat-treated conditions in air and solution was performed, and the better passivation for rolled 304 stainless steel was attributed to its thicker passive film with a higher Cr:Fe ratio [16]. The passive film on type 304 stainless steel in humid atmosphere was characterized with XPS, and the slightly Cr enriched in the passive film under relative humidity 90% was attributed to a thin continuous water layer into which Fe ions were selectively dissolved [17]. By mean of XPS, the compositions of passive layers on AISI 304L and 316L stainless steels after electrochemical oxidation in a borate buffer solution were analyzed as a function of depth of passive layers [6]. The growth of oxide film during anodic polarization in the passive region on 304 stainless steel was studied using XPS [18]. A combination of electrochemical techniques and XPS was used to analyze the behaviour and evolution of passive films generated on AISI 304L for a long immersion time in chloride containing media, it evolved from mixed Fe–Cr magnetite-type structure, and chloride ions did not penetrate into the film that dissolved in a very heterogeneous way [19].

Pitting corrosion of stainless steel is one of classical problems in materials science and electrochemistry. It is well known that pitting corrosion is inevitable for stainless steels in solution containing Cl^-. However, the uniform and pitting corrosion resistances of BN-SS304 were enhanced simultaneously in comparison with CP-SS304 in 0.5 mol/L HCl solution for 30 days' immersion test [20]. The enhanced uniform and pitting corrosion resistances

* Corresponding author. Tel.: +86 24 83978750; fax: +86 24 23891320.
E-mail address: sgwang@imr.ac.cn (S.G. Wang).

0013-4686/$ – see front matter © 2013 Elsevier Ltd. All rights reserved.
http://dx.doi.org/10.1016/j.electacta.2013.09.001

of BN-SS304 resulted from many factors, such as its microstructures, the electronic structures and composition of oxide film on BN-SS304, the dynamic processes of electrode reactions and the properties of electrolyte solution etc. In this work, the electronic structures (core-level binding energies and valence-band structures) and compositions of the two oxide films on BN-SS304 and CP-SS304 were studied by XPS, and the enhanced uniform and pitting corrosion resistances of BN-SS304 were explained according to the electronic structures and compositions of the two oxide films on BN-SS304 and CP-SS304. The two oxide films on BN-SS304 and CP-SS304 after immersion test for 30 days were defined as the two oxide films in this work.

2. Experimental

BN-SS304 was produced by severe rolling technique with CP-SS304 [21,22]. CP-SS304 with $\Phi 40 \times 210\,mm^3$ was annealed at 980 °C for 2 h, and then was rolled as $280 \times 62 \times 15\,mm^3$ sheet by four passes during the temperature of CP-SS304 from 960 to 800 °C. The rolled sheet was cut into two equal parts as $138 \times 62 \times 15\,mm^3$, each cut sheet was rolled as $1230 \times 65 \times 1.6\,mm^3$ by 9 passes during the temperature of CP-SS304 from 700 to 380 °C, and then the final rolled sheet was cooled at room temperature. The total deformation during these processes was about 92%, BN-SS304 can be produced by above processes. The microstructures of BN-SS304 and CP-SS304 were examined with a Philips CM200 transmission electron microscope (TEM) operated at 200 kV and optical microscopy, respectively. The TEM image surface of BN-SS304 is the rolled surface of BN-SS304. The grain sizes of BN-SS304 and CP-SS304 were measured by IMAGE-PRO-PLUS software, they range from 120 to 174 nm and 90 to 120 μm with monomodal distribution, respectively. The average grain sizes of BN-SS304 and CP-SS304 are 150 nm and 100 μm, respectively [22,23], and the chemical compositions of BN-SS304 and CP-SS304 are as follow (at%): carbon <0.0030, silicon <1, manganese <2, phosphorous <0.045, sulphur <0.030, nickel 8–10.5, chromium 18–20, balance iron. BN-SS304 and CP-SS304 specimens for immersion test with size $10 \times 10 \times 1.3\,mm^3$ were abraded using SiC papers of successive grades up to 2000#, cleaned by distilled water, degreased with acetone, and then dried with hair drier. The immersion tests of BN-SS304 and CP-SS304 were carried out in two beakers in 0.5 mol/L HCl solution with 100 mL at room temperature, the time of immersion test was 30 days at room temperature (20 ± 1 °C). During immersion test, the two beakers were covered with paper and were in the place without sunshine. However, the two beakers cannot be sealed up because H_2 will generate from HCl solution during immersion test. The corrosion surface morphologies on BN-SS304 and CP-SS304 for 30 days' immersion were observed by SEM (SSX-550).

The electronic structures and compositions of the two oxide films were characterized by XPS. XPS measurement (Al K_α radiation, $h\nu = 1486.6$ eV) was carried out by an ESCALAB250 surface analysis system. Fermi edge was calibrated using pure Ni and setting the binding energy at 0.00 ± 0.02 eV. Pure Au and Ag standard samples were used to calibrate the binding energy by setting the Au 4f7/2 and Ag 3d5/2 peaks at binding energies of 83.98 ± 0.02 and 368.26 ± 0.02 eV, respectively. The base pressure of ESCALAB250 system was better than 2.8×10^{-10} Pa. The depth profiling on the two oxide films was performed over an area of $2.0 \times 2.0\,mm^2$ under Ar^+ sputtering with 2×10^3 eV. The XPS of different elements in the two oxide films were analyzed with XPSPEAK4.1 software. The atomic percentages of metal atoms (Fe, Cr and Ni), their cations (Fe^{3+}, Fe^{2+}, Cr^{3+} and Ni^{2+}), O_2, Cl^- and O^{2-} along depth profile in the two oxide films were obtained by Ar^+ sputtering for 5050 (for BN-SS304) and 2450 (for CP-SS304) s. The high-resolution spectra of Fe^0 2p3/2, Fe^{2+} 2p3/2, Fe^{3+} 2p3/2, Cr^0 2p3/2, Cr^{3+} 2p3/2, Ni^0 2p3/2, Ni^{2+} 2p3/2, O^0 1s, O^{2-} 1s and Cl^- 2p3/2 in the two oxide films were studied, and then their binding energies along depth profile were provided. The valence electron bands of the two oxide films along depth profile were also obtained by XPS at room temperature. The procedures of specimen preparation, immersion test, SEM observation and XPS characterization of BN-SS304 were the same as those of CP-SS304.

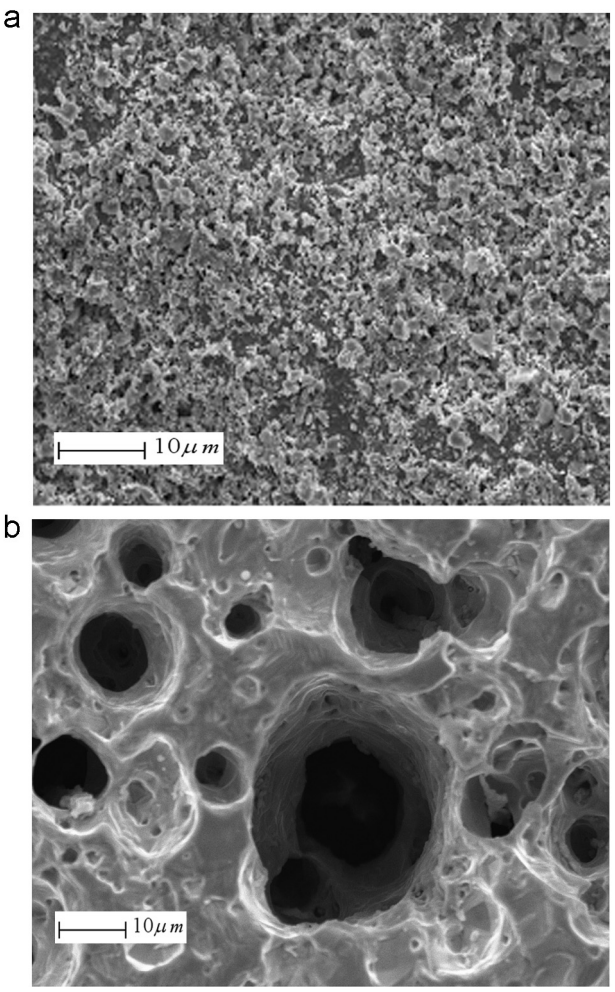

Fig. 1. The corrosion surface morphologies of BN-SS304 (a) and CP-SS304 (b) after 30 days' immersion.

3. Experimental results

3.1. Corrosion morphologies and XPS survey spectra

Fig. 1a and b displays the corrosion surface morphologies on BN-SS304 and CP-SS304 after 30 days' immersion test, respectively. BN-SS304 scarcely suffered from pitting corrosion with the compact oxide film on BN-SS304, while CP-SS304 obviously suffered from pitting corrosion with a number of pits on CP-SS304. Fig. 2 shows the XPS survey spectra of the two oxide films. There were O, Cr, Fe, Ni, Mn and Cl elements in the two oxide films. The analysis of Mn in present work was ignored because it was very difficult to analyze Mn 2p due to the fact that the atomic percentage of Mn was less than 2% and no obvious Mn 2p peaks were observed in present XPS results. Fig. 3 represents the atomic percentages of Cr, Fe and Ni elements in the two oxide films during different Ar^+ sputtering times. The atomic percentages of Fe and Ni elements in the oxide film on CP-SS304 were larger than those on BN-SS304, while the atomic percentage of Cr element in the oxide film on CP-SS304 was

Download English Version:

https://daneshyari.com/en/article/6614922

Download Persian Version:

https://daneshyari.com/article/6614922

Daneshyari.com